物 理 化 学 学 报

*Acta Phys. -Chim. Sin.* **2018,** *34* (X), 0001–0009

[Article] doi: 10.3866/PKU.WHXB201710111 www.whxb.pku.edu.cn

# Chemical Bonding and Interpretation of Time-Dependent Electronic Processes with Maximum Probability Domains

SAVIN Andreas*

Laboratoire de Chimie Théorique, CNRS, and Sorbonne Université, UPMC Univ Paris 06, 4 place Jussieu, F 75252 Paris cedex 05, France.

**Abstract:** Tools have been designed obtain information about chemical bonds from quantum mechanical calculations. They work well for solutions of the stationary Schrödinger equation, but it is not clear whether Lewis electron pairs they aim to reproduce survive in time-dependent processes, in spite of the underlying Pauli principle being obeyed in this regime. A simple model of two same-spin non-interacting fermions in a one-dimensional box with an opaque wall, is used to study this problem, because it allows presenting the detailed structure of the wave function. It is shown that i) oscillations persisting after the Hamiltonian stopped changing produce for certain time intervals states where Lewis electron pairs are spatially separated, and ii) methods (like density analysis, or the electron localization function) that are widely used for describing bonding in the stationary case, have limitations in such situations. An exception is provided by the maximum probability domain (the spatial domain that maximizes the probability to find a given number of particles in it). It is conceptually simple, and satisfactorily describes the phenomenon.

**Key Words:** Chemical bond; Time-dependent Schrödinger equation; Particle in a box with opaque wall

## 1 Introduction

Many tools have been developed to describe chemical bonding using quantum mechanics. But chemical bonding changes during structural modifications of the molecules. Does assigning spatial domains to electron pairs (the Lewis perspective) survive in time-dependent processes? Usual chemical routine uses curved arrows, suggesting that this is the case. Quantum chemical calculations performed along the reaction path tend to confirm it. But is this adiabatic picture correct?

This paper uses a simple model, of two independent particles of the same spin, in a one-dimensional box. (As the formation of the Lewis pairs is mainly due to the Pauli principle, and only independent particles are discussed in this paper, the treatment of two electrons of the same spin is easily transposed to the treatment of two electron pairs.) At start, each of the the particles is confined to a half-box. The wall between boxes becomes transparent with time, allowing the particle to pass from one half-box to the other. After some time, $\tau$, the wall completely disappears.

Using a "reasonable" definition, one can attribute a spatial domain to one of the electrons, the other one being in the remaining space available. This evidently works when the wall is impenetrable. One may naively believe that making the separation wall vanish does not qualitatively change the situation, that the Pauli principle forces the two electron pairs to remain as such, whether they are separated by a wall, or not. However, as we consider a model for a chemical reaction, we should look at the influence of time on the electron localization domain, and whether it affects our perception of electron localization.

The time evolution is computed using

(1) the adiabatic approximation, valid when the Hamiltonian changes very slowly with time,

(2) the sudden approximation, valid when the change of the Hamiltonian is fast,

(3) an explicit solution of the time-dependent Schrödinger equation, for a finite basis set, and given parameters of the system.

For a more precise definition of "slow" and "fast", see, e.g.[1], section XVII.

The calculations below show that with the last two approaches, for certain time intervals, electrons are not essentially confined to the half-boxes, in contrast to a Lewis-like concept. One can find that one electron (or electron pair) is located in the center of the box, while the other is delocalized over the remaining left and right parts.

The simplicity of the model allows presenting the detailed

---

Received: September 1, 2017; Revised: September 25, 2017; Accepted: September 25, 2017; Published online: October 11, 2017.

*Corresponding author. Email: andreas.savin@lct.jussieu.fr.

structure of the wave function. Pictures are presented using other interpretative tools that can also be used for more complicated systems (localized orbitals, the density, and its second derivative, the electron localization function, and the maximum probability domains). It is concluded that the latter method is preferable to describe time-dependent processes, although one should keep in mind that the present calculations are far from being representative for real systems.

## 2 System

### 2.1 Hamiltonian

A one-dimensional box stretching from $-L$ to $L$ is separated at $x = 0$ by an opaque wall (see, e.g.[2], problems 19, 20). The potential is given by:

$$v(x,t,L) = a(t)\delta(x) \text{ if } L < x < -L \tag{1}$$

and is infinite outside this interval. The parameter $a$ defines the "opacity" of the wall. For $a = 0$ there is no separation between the two half-boxes (corresponding to $x < 0$, and $x > 0$, respectively). For $a = \infty$ there is no communication between them: the wall at $x = 0$ is impenetrable, and each electron is confined to its half-box. In this paper we consider that the opacity parameter $a$ can change with time, $t$. To simplify notation, $L$ is dropped when equal to 1.

### 2.2 Stationary solutions

The solution of the stationary Schrödinger equation for this potential is analytically known. By the symmetry of the potential $v(x)$, there are two types of solutions,

symmetric, $u_+(x) = u_+(-x)$, and
antisymmetric, $u_-(x) = -u_-(-x)$.

The antisymmetric solutions have a node at $x = 0$, and are thus not affected by the term $a\delta(x)$ appearing in $v(x)$, Eq.(1). The explicit forms of $u_\pm$ are given in Appendix A. Fig.1 shows $u_+(n = 1, x, a)$, and $u_+(n = 2, x, a)$ for different values of the parameter $a$, as well as $u_-$ for $n = 1, 2$. Please notice the notch in $u_+$ produced by $a\delta(x)$ becoming more pronounced as $a$ increases (at given $n$).

### 2.3 A triplet non-interacting two particle system

The model system studied in this paper consists of two non-interacting fermions, in a triplet state. In fact, it stands for a system for two non-interacting electron pairs in a singlet state. Having another two electrons with opposite spin changes little to the problem, as the anti-symmetrization needs to be done only among particles of the same spin. The properties of this non-interacting system can be computed from a wave function that is a product of two identical two-by-two Slater determinants, one for each spin (see, e.g.[3]). It is thus sufficient to analyze only one of them, the properties of the four-electron system being understood easily from those of the same-spin two electron system. For example, if we have the density of the system with two spin-up electrons in the triplet state, we just have to multiply it by two to obtain that of the four-electron system.

The repulsion between electrons has been neglected because the formation of electron pairs is not due to electron repulsion. The intuition of Lewis was that Coulomb's law is not valid at short distances, and that "each pair of electrons has a tendency to be drawn together"[4]. Although the explanation given by Lewis is not correct, such an effect is seen in mean-field models like Hartree-Fock; localized orbitals with different spin are pairwise identical in the spatial part. It is the Pauli principle that keeps the electrons with same spin apart, and it acts whether or not they interact. Opposite spin electrons can share the same spatial domain, and can form the pairs described by Lewis. In fact, many of the tools used to analyze the chemical bond only exploit the Pauli principle.

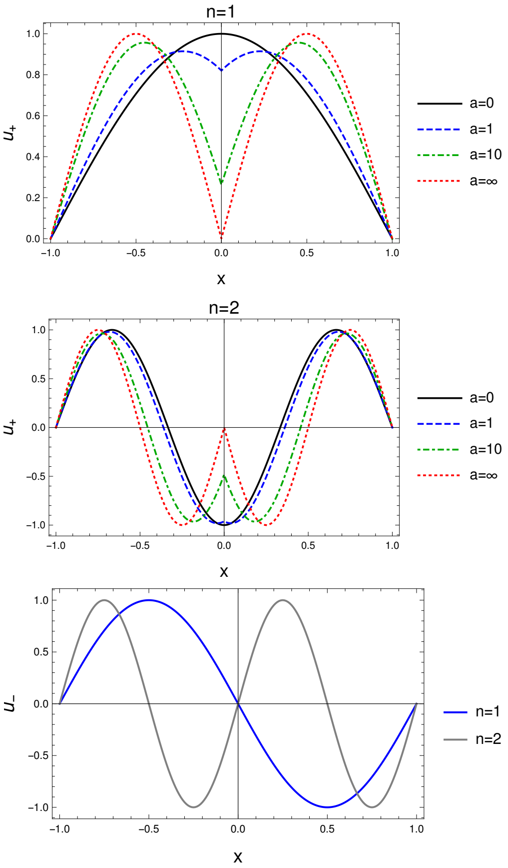

**Fig.1 One-particle eigenfunctions of the stationary Schrödinger equation for a particle in a box with an opaque wall; symmetric solutions $u_+$, for $n = 1$ (top), for $n = 2$ (center), for different values of the opacity parameter $a$, and antisymmetric solutions $u_-$ (bottom), for $n = 1, 2$.**

Another reason not to introduce repulsion in the present calculations is that there is not a clear way how repulsion should be treated in one dimension. The Coulomb interaction in one dimension, $1/|x_1 - x_2|$ produces a severe singularity at $x_1 = x_2$, and the volume element does not make it vanish, as it does in three dimensions. Softened Coulomb repulsion has to be used (see, e.g.[5]). Physically, this is easy to understand: electrons can better avoid each other in three dimensions than in one dimension.

### 2.4 Analogies

In order to see a connection to chemistry, we can imagine some analogue. For example, one could consider two He atoms getting closer. From the Lewis pairing perspective, nothing interesting can be expected: even for $\mathrm{He}_2$, the electron pairs stay on each of the atoms.

In analogy to a molecule formation in time, we start with the particles separated by an infinite wall, $a = \infty$ (or, with a very large value). As time evolves the opacity parameter $a$ goes to zero so that the particles finally do not see a wall at $x = 0$, and can move freely in the whole box, from $-L$ to $L$.

## 3 Tools to analyze the electron distribution

There are many tools to analyze the electronic structure. Just a few are used below, and are now shortly described.

### 3.1 Wave function

One can analyze the wave function. In general, it has a too high dimension. For our example, it is only in two dimensions (the coordinate of each of the particles), and can be easily plotted.

In order to avoid the dimensionality problem, Artmann[6] proposed to locate the maxima of the wave function. This is a very appealing proposal, well adapted to method like Quantum Monte Carlo[7]. It has the disadvantage that the wave function can present several maxima, and one has to choose among them. This can be avoided in many practical situations by choosing a domain around them[8].

### 3.2 Maximum probability domains

One way to define a spatial domain is to consider the one that maximizes the probability to have a given number of particles, $\nu$, in it[9], the "maximum probability domains" (MPDs). In our example, we search for a domain $\Omega$, such that the probability to find one (and only one) particle in it

$$p(\nu = 1, \Omega) = N \int_{\Omega} \mathrm{d}^3 r_1 \int_{R^3 \setminus \Omega} \mathrm{d}^3 r_2 ... |\Psi(r_1, r_2, ..)|^2$$

is maximal. $\int_{\Omega}$ means that the integration is performed only over $\Omega$ that may, but must not be spatially disconnected; the prefactor $N$, the number of particles in the system, is due to the indistinguishably of electrons.

### 3.3 Density

A simple three-dimensional quantity is the electron density, $\rho$,

$$\rho(r_1) = N \int \mathrm{d}^3 r_2 ... |\Psi(r_1, r_2, ..)|^2$$

Its analysis and use has been much promoted by Bader[10]. The particle density should not be confused with a probability density, as

$$\int_{\Omega} \rho(r)\, \mathrm{d}^3 r \neq p(\nu = 1, \Omega)$$

This integral over the density gives the average number of particles in $\Omega$.

### 3.4 Second density derivative

The maxima of $-\nabla^2 \rho$ are used to indicate where electron pairs localize (see, e.g.[10], section 7.1.4). Here, as our system is in one dimension, $-\partial_x^2$ is used.

### 3.5 Electron localization function

Another popular quantity to detect the Lewis pairs is the electron localization function (ELF)[11]. It is a function defined in each point of space, takig values between 0 and 1. For regions where electrons localize, the values of ELF should be large. It has been generalized to time-dependent processes, TDELF[12]. In this paper, we use a formula that is modified for particles in one dimension. The explicit expression of ELF is given in the Appendix B.

As we deal with independent particles, we do not have to worry about generalizations of ELF for wave functions beyond a single Slater determinant.

### 3.6 Localized orbitals

Localized orbitals provide a simple interpretation tool, and are also be used below. For example, for the stationary lowest energy solution, the localized orbitals are just the linear combination of the two lowest energy canonical orbitals with different symmetry, $[u_+(n = 1, x, a) \pm u_-(n = 1, x, a)]/\sqrt{2}$. Inversion, $x \to -x$, transforms one localized orbital into the other.

## 4 Results

### 4.1 Hamiltonian changes slowly with time

Let us first consider systems where the Hamiltonian changes slowly with time. In this case, one can simply use the solutions of the stationary Schrödinger equation, at each moment $t$. This is the most widely used treatment. For example, one solves the Schrödinger equation on points on the reaction path, and uses one of the bonding interpretation tools available.

Corresponding to this image, it is sufficient to present pictures obtained for different values of the opacity parameter $a$. To get an order-of-magnitude idea of how $a$ changes with time, see Appendix C.

As expected, our system turns out to be uninteresting. All the methods mentioned above give the same result that can be summarized as "one electron in each of the half-boxes", at all times. Of course, this statement is strict when $a = \infty$, and is only qualitatively valid when $a$ is finite. Fig.2 shows that only the extreme cases, when there is an impenetrable wall separating the half-boxes ($a = \infty$), and when there is no separation ($a = 0$). A discussion of this figure follows, in order to prepare that of the following section, when a new situation shows up.

The wave function, for $a = \infty$, is strictly localized in each of the half-boxes (it is zero when $x_1$ is in one half-box, and $x_2$ in the other). When the wall is removed, the wave function slightly extends over the other half-box (Fig.2a).

In accordance with it, the perfectly localized orbitals for $a = \infty$, slightly delocalize, even for $a$ down to 0 (Fig.2b).

The density shows two peaks, each centered in a half-box; $-\partial_x^2 \rho(x)$ has also such maxima (Fig.2c and Fig.2d).

ELF takes the maximal value ($= 1$) when the half-boxes are separated, and each of the electrons is localized in one of them (Fig.2e). When $a = 0$, ELF decreases, but only in the wall region, showing again the localization of particles in the half-boxes.

Fig.2f shows the probability of finding one electron between $x_<$ and $x_>$. When the spatial region $x \in (x_<, x_>)$, is chosen to maximize the probability to find one, and only one particle in it, two solutions are found: $x_< = -L, x_> = 0$, and $x_< = 0, x_> = L$. A maximum probability domain is thus either the segment corresponding to the left, or that corresponding to the right half-box.

## 4.2 Sudden change of the Hamiltonian

### 4.2.1 Mathematical description

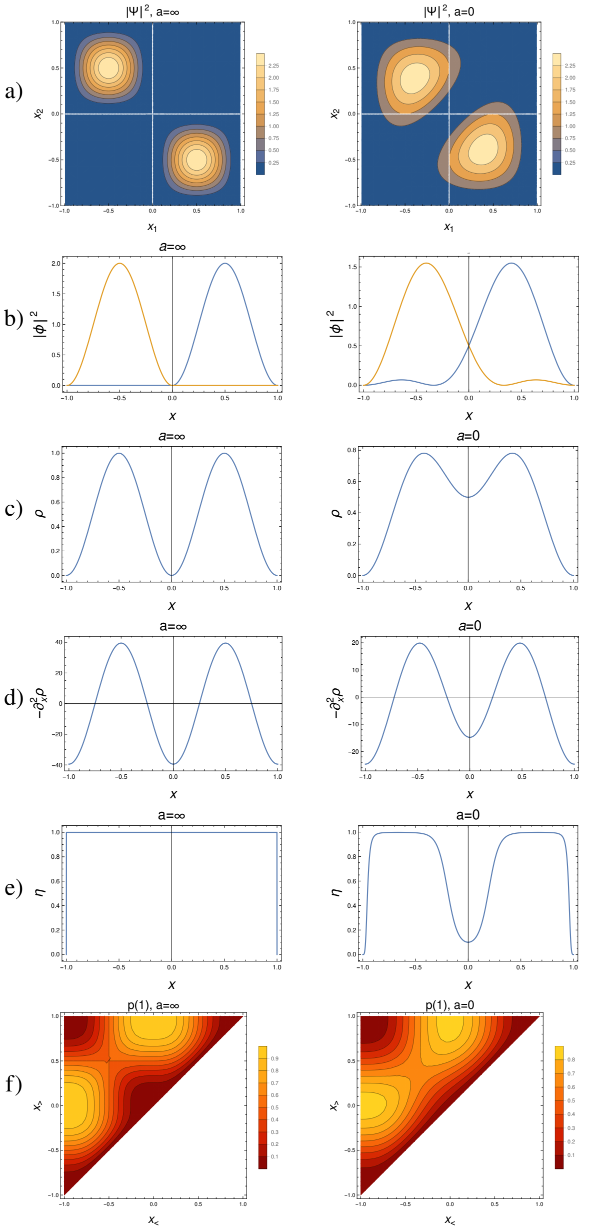

**Fig.2 Slow change of the Hamiltonian with time. From top to bottom: a) absolute value of the wave function squared, as function of the coordinates of the particles, $x_1, x_2$, b) localized molecular orbitals, c) density, d) minus the second derivative of the density, e) the electron localization function, f) the probability to find one, and only one electron between $x_<$ and $x_>$; left: impenetrable wall ($a = \infty$), right: wall has vanished ($a = 0$).**

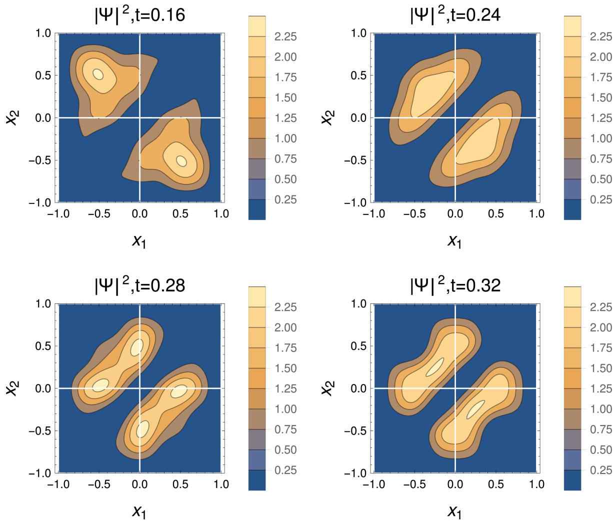

**Fig.3 Absolute value of the wave function squared, for a sudden change of the Hamiltonian as a function of the coordinates of the particles, $x_1, x_2$. The time after the change of the Hamiltonian is given in atomic units (1 a.u. ≈ 24 attoseconds), for $L = 1$.**

We consider now the opposite extreme, when the modification in time occurs with a jump, from the Hamiltonian with $a = \infty$ to that with $a = 0$. We recall that all the $u_-$ states are unaffected by the perturbation (that is present only at the node of these functions). After the Hamiltonian has changed, $u_+(n = 1, x, a = \infty, L)$ is not the ground state anymore. We expand the initial state, $u_+(n = 1, x, a = \infty, L)$ on the final states, $u_+(k, x, a = 0, L)$,

$$\varphi_+(n=1,x,L,t) = \sum_k \langle u_+(k,x,a=0,L)|u_+(n=1,x,a=\infty)\rangle \, u_+(k,x,a=0,L)\mathrm{e}^{-iE(k,a=0,L)t} \qquad (2)$$

This expression shows how excited states of the stationary Schrödinger equation for the final Hamiltonian participate to the wave function $\varphi_+$.

### 4.2.2 Wave function

The evolution of the square of the two-particle wave function with time is presented in Fig.3. The starting point ($t = 0$) is that shown for $a = \infty$ in Fig.2. At the very beginning of the process each of the particle remains highly localized in its half-box. However, the particles "realize" that they have more space at their disposal, and start to expand ($t = 0.16$). A broad maximum appears later ($t = 0.24$), and its nature is understood a short time later ($t = 0.28$). The wave function has maxima at $x_1 = 0$, $x_2 \approx 0.5$, etc.: while one of the particles is in the center of the box, the other particle can be in either of the half boxes. This is followed, by another broad maximum ($t = 0.32$), followed by again a situation as for $t = 0.28$, etc., until the particles retract to the initial half-boxes, and the process starts again.

### 4.2.3 Localized orbitals

Localized orbitals for this process are shown in Fig.4. The orbitals delocalize into the other half-box ($t = 0.24$). During this process the orbitals get very close to each other ($t = 0.28, t = 0.32$), before reversing the movement, going back to the original

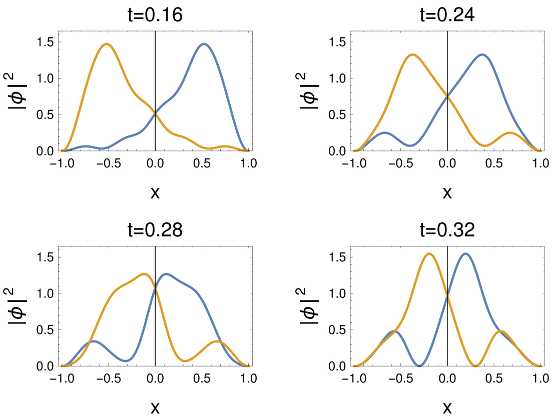

**Fig.4** **Absolute value of the square of the localized orbitals, for a sudden change of the Hamiltonian. The time after the change of the Hamiltonian is given in atomic units (1 a.u. $\approx 24$ attoseconds), for $L = 1$.**

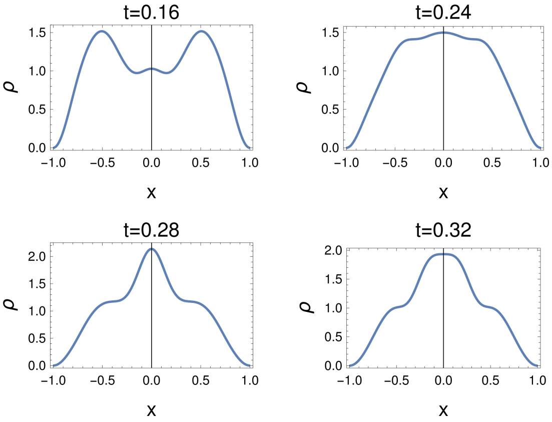

**Fig.5** **Density, $\rho$, for a sudden change of the Hamiltonian. The time after the change of the Hamiltonian is given in atomic units (1 a.u. $\approx 24$ attoseconds), for $L = 1$.**

half-box, and restarting the cycle. It is worth to remark that in the "unconventional", intermediate step ($t \approx 0.3$), the centroids of charges of the two localized orbitals get much closer than at the start: the localization is only poorly realized. We will later come back to this point.

### 4.2.4 Density

The change of the density compresses what has been seen above, and some information can be lost, cf. Fig.5. At $t = 0.16$ the density presents two important peaks, as could be expected, but a new small maximum shows up in between. The latter reminds of the so-called "non-nuclear attractors" that are associated to metallic systems (see, e.g. [10], section E2.1.1). At $t = 0.24$, in accordance with the broad maximum in the wave function, there is a broad maximum in the density. At later times ($t = 0.28, 0.32$), the density has a central maximum, and shoulders appear instead of the outer maxima. Plots of the density are not expected to show such features in the stationary case.

### 4.2.5 "Laplacian" of the density

Instead of the Laplacian of the density we consider again, as suited to the one-dimensional problem, $-\partial_x^2\rho$. The problems in interpreting the density get magnified, cf. Fig.6. For example, the small maximum in the density at $t = 0.16$ gets similar importance to the other two. At $t = 0.24$ the difference between maxima fades. At $t = 0.32$, four maxima show up. Should one relate them to the two maxima in each of the localized orbitals? As with the density, one can speculate about the origin of these maxima, once we have more information, but can we interpret $-\partial_x^2\rho$ without having it? The problem of having too many maxima reminds of one known for the CC bond in ethane, see, e.g. [10], section 3.2.4). There, although there is just one bond and one would expect a single maximum, the Laplacian of the density shows two maxima.

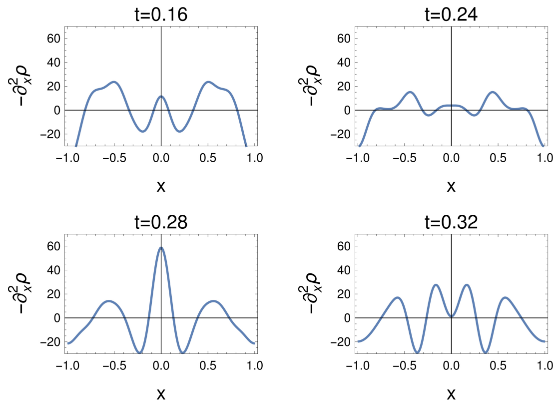

**Fig.6** **$-\partial_x^2\rho$, for a sudden change of the Hamiltonian. The time after the change of the Hamiltonian is given in atomic units (1 a.u. $\approx 24$ attoseconds), for $L = 1$.**

### 4.2.6 Electron localization function

The electron localization function brings in information that is consistent with the information the $\psi(x_1, x_2)$ gives. The graphs show more clearly what is happening than $-\partial_x^2\rho$, as for all $t$ shown, at most three maxima show up (see, Fig.7). One is very weak at $t = 0.16$, is weakly distinguishable from the others at $t = 0.24$, while three clear maxima show up clearly at $t = 0.28, 0.32$. However, as for $-\partial_x^2\rho$, it is hard to guess what three maxima mean, when only two electrons are present, because ELF is used to attribute a domain to each of the electrons (or electron pairs). Knowing that one electron is delocalized over two spatial regions solves the problem. However, one should know that the two basins (on the left, and on the right) have to be grouped together. One could integrate the density over these regions (these basins), and get $\approx 3/4$ electrons in it. One should note, however, that, oscillations occur (see below), and some further criteria to unify the newly appeared basins are needed.

### 4.2.7 Maximum probability domain

For interpretation reasons, the maximum probability domains seem to have the simplest structure. Fig.8 shows the probabilities to find one electron between $x_<$ and $x_>$. In these pictures we search for the pairs $x_<$ and $x_>$ that correspond to the maximum probability. The segment $(x_<, x_>)$ is a domain for which the probability to find one and only one electron is maximal. If only one electron is in this segment, the other one has to be in the remaining region between $-L$ and $L$. Of course, when

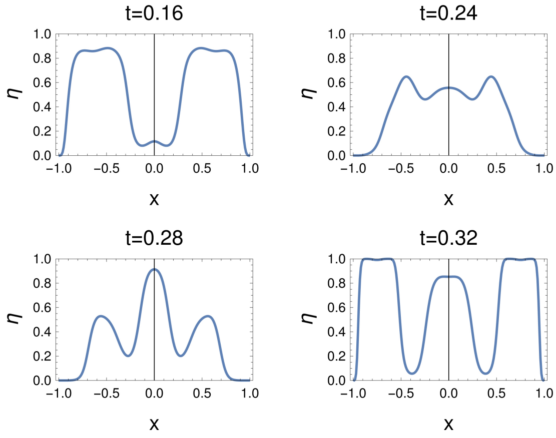

**Fig.7** **Electron localization function, $\eta$, for a sudden change of the Hamiltonian. The time after the change of the Hamiltonian is given in atomic units (1 a.u. ≈ 24 attoseconds), for $L = 1$.**

$x_< \neq -L$, or when $x_> \neq -L$, the latter is disconnected; it is the union of $(-L, x_<)$ and $(x_>, L)$.

At $t = 0.16$, the two half-boxes are the maximum probability domains. However, at $t = 0.24$, a difference to the adiabatic picture is clear. For any fixed $x_<$ chosen, one can find a value $x_<$ such that the probability to find an electron in this segment is maximal. Surprisingly, the maximal value is almost independent of the chosen $x_< \in (-L, L)$. At $t = 0.28, 0.32$, a single maximum shows up. It corresponds to a central maximal probability domain, and one covering the remaining part of the box (left and right of it).

### 4.2.8 Physical interpretation

Eq.(2) is valid when the change of the Hamiltonian is so fast that the wave function does not have the time to change. After the change, the wave function $\varphi$ evolves with time, and to 98 percent is a mixture of the $u_+(n = 1, a = 0, x)$ and $u_+(n = 2, a = 0, x)$ states (Rabi oscillations are produced):

$$|\varphi_+|^2 = c_1^2 u_1^2 + c_2^2 u_2^2 + 2c_1c_2u_1u_2\cos(\Delta E t) + \ldots \tag{3}$$

where $u_k = u_+(n = k, x, a = 0)$, $\Delta E = \pi^2$ is the difference between the energies of the $n = 2$ and $n = 1$ states, $c_1 = 8/(3\pi)$, $c_2 = 8/(5\pi)$. The extreme cases occur when the cosine function equals plus or minus one, i.e., at $t = jT$ and $t = (j + 1/2)T$ where $j$ is an integer number, $T = 2\pi/\Delta E = 2/\pi$.

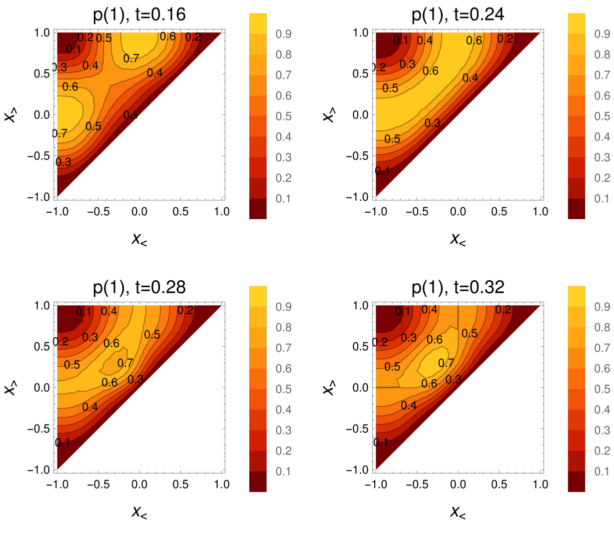

**Fig.8** **Probability to find one, and only one electron between $x_<$ and $x_>$, for a sudden change of the Hamiltonian. The time after the change of the Hamiltonian is given in atomic units (1 a.u. ≈ 24 attoseconds), for $L = 1$.**

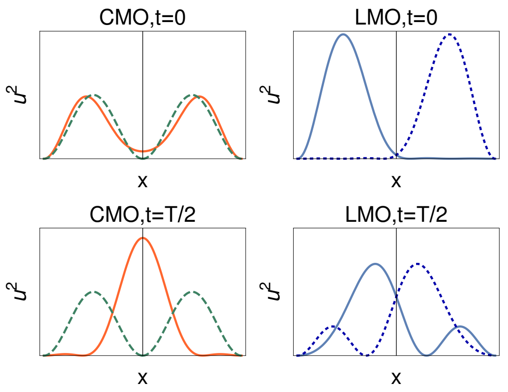

**Fig.9** **Time-dependent orbitals squared, reduced to the $n = 1, 2$ components, at times $t = 0, T, \ldots$ (upper panels), and $t = T/2, 3T/2, \ldots$ (lower panels); left for symmetry-adapted orbitals (full lines: $u_+$, dashed lines: $u_-$), right for localized orbitals; same scale in all panels.**

Fig.9 shows the squares of the orbitals for times equal to even or for odd numbers of $T/2$. One notices that at $t = 0$, the occupied canonical orbitals squared are similar. The difference between them comes mainly from the sign in one of the half-boxes. This allows an almost perfect localization by linearly combining the canonical orbitals. In contrast to it, at $t = T/2$, the symmetric orbital is well localized at the center of the box, while the antisymmetric one, $u_-$, is unchanged. The localization obtained by linearly combining the canonical orbitals is poor: the centroids of the orbitals are close, the delocalization is strong. The total wave function $\psi(x_1, x_2, t = T/2)$ is given by the Slater determinant built from $\varphi_+$ and $u_-$. It has maxima for $x_1 = 0$, and $x_2 = \pm 0.5$. $\psi$ is not shown, as it resembles the one of Fig.3. One can understand it by noticing that $u_- = 0$ where $\varphi_+$ has a maximum, and $\varphi_+$ almost vanishes where $u_-$ has extrema. The picture produced by the canonical orbitals (one strongly localized orbital, and one delocalized orbital) is closer to the one obtained by looking directly to the total wave function than the one produced by the two poorly localized orbitals.

The maximum probability domains do not start from an orbital "prejudice", but analyze the total wave function. After the separating wall has vanished, for certain intervals of time, there is a maximum probability domain around the position where the wall has been. Also, by permitting the spatial region to be spatially disconnected, they allow for the description of the quantum phenomenon that a particle can be found in two different disconnected domains.

### 4.2.9 Comparison to stationary states

The best description of the chemical bond is not necessarily given by a single localized solution even when considering the time-independent case. The simplest example is the $H_2^+$ molecule, where a localized solution does not exist. One may have a localized picture by using resonance structures. In the case of $H_2^+$, one can describe it as H . . . $H^+ \leftrightarrow H^+$. . . H. For the system considered in this paper, one can imagine the state at $t = T/2$ as

$$\uparrow \dots \uparrow \; \cdots \circ \leftrightarrow \circ \dots \uparrow \dots \uparrow$$

where $\circ$ denotes an unoccupied site. One electron stays at the center, while the other can be either in the left, or in the right half-box. (Of course, as stated before, the single electron $\uparrow$ can be replaced by a pair $\uparrow\downarrow$. The left or right location of the electron pair reminds of the ionic resonant state of $H_2$, or the charge-shift (resonating) bond[13].)

Another example is given by particles in a ring, or metals, where the localization is not considered to give the best description. Let us assume that for particles in a ring we have found some region, defined by the points $x_<$ and $x_>$, such that the probability to find $\nu$ particles reaches a maximum. Displacing both points by some constant value $\kappa$ defines a new region. By translational invariance, the probability to find $\nu$ particles in it is independent of $\kappa$. Of course, changing just one of $x_<$, or $x_>$ lowers the probability. This behavior is analogous to what is seen in Fig.8, $t = 0.24$: pairs of $x_<$ and $x_>$ for which there is practically no change in the probability.

One more example is given by atomic shells. Although, e.g., in an atom like Ne there are four electron pairs, due to spherical symmetry a spatial region defining an electron pair can be oriented in any direction: there are infinitely many equivalent "pair domains". In this case, we consider atomic shells, and only destroying the symmetry fixes the orientation of the pairs.

It is worth to stress that in the time-dependent case discussed in this paper, it is not the symmetry that produces equivalent solutions, but the mixing with excited eigenstates that generates different localization patterns.

Interestingly, Lewis[4] had the intuition of the failure of taking his model rigidly. Although desiring to explain polarity, and not the quantum effects discussed here, he writes about "tautomerism, where two or more forms of the molecule pass readily into one another and exist together in a condition of mobile equilibrium".

#### 4.2.10 Period of the cycle

For $L = 1$, the symmetric orbital $\varphi_+$ changes with a period $T \approx 0.64$ atomic units, or $\approx 15$ attoseconds. This mainly due to the separation between the two lowest energy levels, $E(n = 1, a = 0)$, and $E(n = 2, a = 0)$, of the symmetric states $u_+$. As $E(k, a = 0, L) = E(k, a = 0, L = 1)/L^2$, the time evolution for $L \neq 1$ is easily recovered *via* the transformation $t \rightarrow tL^2$. The difference between $E(n = 2, a = 0)$ and $E(n = 1, a = 0)$ that determines the period of the oscillations, is unrealistically large for $L = 1$ ($\approx$ 10 hartree). This can be corrected by choosing a larger box. For example, by choosing $L = 10$, it is brought down to $\approx 0.1$ hartree, or $\approx 3$ eV. This way, the period of the cycle is of 1.5 femtoseconds.

#### 4.2.11 Spatial oscillations

Up to now, an important technical detail was hidden from the discussion, viz., the number of functions $u_+(k, x, a = 0)$ used in Eq.(2). As the process analyzed above is determined mainly by the two lowest energy symmetric states, the figures were produced by limiting the sum to $k \leq 5$. We can analyze the effect of increasing the number of functions, e.g., up to $k = 10$. ELF, and even more importantly $-\partial_x^2\rho$ emphasize the rapid oscillations produced by adding these higher frequency components. These rapid oscillations produce many maxima, and this makes any analysis based on counting the maxima useless. However, almost no effect is seen on the probabilities. This can be understood by the need of taking derivatives for obtaining $-\partial_x^2\rho$ , while integration used for generating the probabilities has a smoothing effect.

### 4.3 Explicit solution of the time-dependent Schrödinger equation

#### 4.3.1 Mathematical description

Up to now, we have obtained results in two limiting cases. We would like to know whether the sudden approximation may be relevant. For this, let us consider expand the time-dependent, spatially symmetric wave function as

$$\phi_+(x,t) = \sum_n c_n(t)\chi_n(x) \tag{4}$$

After substitution of $\phi_+$ into the time-dependent Schrödinger equation, and projection on $\chi_m(x)$, we have

$$i\,\dot{c}_m(t) = \sum_n c_n(t) \int dx\,\chi_m(x)\,H(x,t)\,\chi_n(x) \tag{5}$$

where the dot above the letter represents the derivative with respect to $t$.

Details on solving this equation are given in Appendix D.

In contrast to the treatment before, we cannot start at $t = \infty$, because we would need infinite time to follow the evolution. Furthermore, we have to decide about how the opacity parameter $a$ changes with time. $a$ is uniformly switched off from a large value, in $\tau \approx 10$ femtoseconds. For $t > \tau$, the Hamiltonian does not change with time anymore, but the wave function continues to evolve according to the Schrödinger equation, having as initial wave function $\phi_+(\tau, x)$. Details on the choice of the parameters can be found in Appendix C.

#### 4.3.2 Probability evolution

If the change of the opacity parameter $a$ with time were very slow, one would see essentially the same images as in Fig.2. However, for the choice of the parameters just described, the results look similar to those given for the sudden approximation. It is thus not necessary to show and analyze in detail the results again. The calculation has only shown that the regime of the sudden approximation is not unrealistic.

Nevertheless, we discuss how the probabilities evolve with time (see Fig.10). One of the curves corresponds to the probability of finding one electron in a half-box. The other, to that of finding one electron in the center (equal to that of

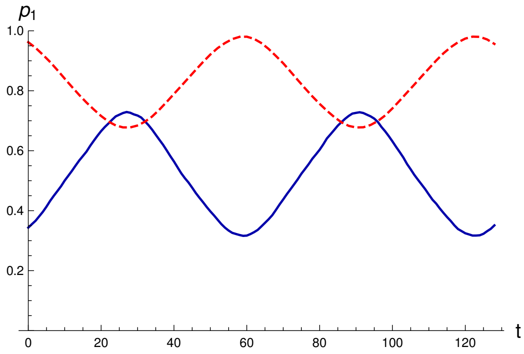

**Fig.10 Probability to find one, and only one electron in a half-box (between $x_< = 0$ and $x_> = L$), dashed curve, and that for $x_< = 0.3L$ and $x_> = 0.3L$ (full curve), as a function of time after the Hamiltonian stopped changing (given in atomic units, 1 a.u. $\approx$ 24 attoseconds; for $L = 10$, and the the wall made transparent in $\tau \approx 10$ femtoseconds).**

finding one electron in the disconnected domain that excludes this central region). In Fig.10, when following the evolution in the central region, $x_< = -x_>$ was arbitrarily set to a time-independent constant. The optimization of $x_<, x_>$ increases the probability, and moves up the curve in the figure.

Although the probability to find a central MPD is not large at the moment $\tau$, when the Hamiltonian has arrived at the final form, one notices that the probabilities continues to change in time, with periods of $\approx$ 64 a.u. ($\approx$ 1.5 femtoseconds). Furthermore, the variation with time is important. For $\approx 1/6$ of the cycle, around the the probability of finding one electron in the central region is larger than that of finding one in a half-box. The duration where the two probabilities are comparable is even more important.

## 5 Perspectives

The example of two electrons with the same spin shows that when the Hamiltonian changes electron localization may look, for certain time intervals, qualitatively different from what the adiabatic picture presents. In our example, the latter follows that of Lewis, while time dependence brings in quantum delocalization effects. It gives a significant probability of finding an electron in two spatially disconnected regions.

An analogue to the spatially disconnected regions exists for the wave function solving the stationary Schrödinger equation, e.g., when resonant structures are needed to describe the bonding. It can be speculated that phenomena like this play a role, e.g., in charge transfer, in transport properties, also in nano and biological systems.

One should not forget that two particles in a box with an opaque wall do not represent reality, and that no choice of the parameters of the model can compensate for it. However, the simplicity of the model allows us to look at the wave function, and understand better how well, or how badly, the interpretation tools work. Thus, the paper has only two objectives, namely to encourage

- the study of time-dependent processes, as they disclose unexpected situations for chemical bond description, and
- the use of the maximum probability domains that seem well suited for such time-dependent processes.

We finally mention that latter is close to what is already used in time-dependent context, see, e.g.[14], and that limitations of ELF in time-dependent cases has also been noted before[5].

## 6 Dedication

This paper is dedicated to Debashis Mukherjee, who reached his seventies birthday. During the many years of our friendship we spent a long time in discussions on various subjects, including that of the present paper.

## Appendix

### A Solutions of the stationary Schrödinger equation for a particle in a box with an opaque wall

As given in Ref.2 (problems 19,20), the expressions of the one-particle wave functions, solutions of the stationary Schrödinger equation with potential $v(x)$ given in Eq.(1), are given by

$$u_-(n,x,L) = \begin{cases} 0 & \text{if } x \leq -L \\ \frac{1}{\sqrt{L}} \sin[\frac{n\pi}{L}(x+L)] & \text{if } -L < x < 0 \\ \frac{1}{\sqrt{L}} \sin[\frac{n\pi}{L}(x-L)] & \text{if } 0 \leq x < L \\ 0 & \text{if } L \leq x \end{cases} \tag{6}$$

and by

$$u_+(n,a,x,L) =$$

$$\begin{cases} 0 & \text{if } x \leq -L \\ A(n,a,L)\sin[k(n,a,L)(x+L)] & \text{if } -L < x < 0 \\ A(n,a,L)\sin[k(n,a,L)(x-L)] & \text{if } 0 \leq x < L \\ 0 & \text{if } L \leq x \end{cases} \tag{7}$$

where $k(n,a,L)$ is the solution of

$$k(n,a,L)\cot[k(n,a,L)L] = -a$$

lying between $(n-1/2)\pi/L$ and $n\pi/L$. The normalization constant is

$$A(n,a,L) = \sqrt{\frac{2k(n,a,L)}{2k(n,a,L)L - \sin[2k(n,a,L)L}}$$

Notice that $u_+$ does not change sign with $x \to -x$, while $u_-$ does.

The eigenvalues are given by

$$E(n,a,L) = \frac{1}{2}k(n,a,L)^2/L^2$$

Their dependence $a$ is shown in Fig.11.

### B The expression of the electron localization function for a single Slater determinant

As we are discussing one-dimensional systems, the formula of ELF is slightly different from that generally used. Also, we consider the fully polarized systems, while usually the closed-shell formula is given. We follow the initial choice of the interpretation of ELF[11], viz. related to the curvature of the

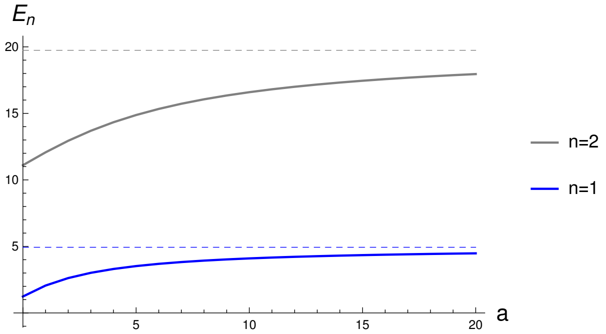

**Fig.11 Eigenvalues of the stationary Schrödinger equation for a particle in a box with a wall having an opacity increasing with $a$; for $n = 1, 2$; those corresponding to the symmetric eigenfunctions $u_+$ are shown with full lines; those of the antisymmetric eigenfunctions $u_-$ do not depend on $a$ and are shown as horizontal dashed lines.**

Fermi hole. It also includes the current contribution[15], as needed when orbitals are complex, as is the case in time-dependent theory[12]. For a single Slater determinant, the explicit expression of ELF is

$$\eta(x) = \frac{1}{1 + [D(x,t)/D_{UEG}(x,t)]^2}$$

where

$$D(x,t) = \xi(r,t) - \frac{1}{8}\frac{|\partial_x \rho(x,t)|^2}{\rho(x,t)} - \frac{1}{2} j(x,t)$$

$$\rho(x,t) = \sum_n |\phi_n(x,t)|^2$$

$$\xi(x,t) = \frac{1}{2}\sum_n |\partial_x \phi_n(x,t)|^2$$

$$j(x,t) = \frac{1}{2i}\sum_n \phi_j^*(x,t)\partial_x\phi_n(x,t) - \phi_n(x,t)\partial_x\phi_n^*(x,t)$$

$\phi_n$ are the occupied orbitals of the Slater determinant, $D_{UEG}$ is the expression of $D$ computed for the one-dimensional uniform electron gas of density equal to $\rho(x,t)$

$$\xi(x,t) \to \tau_{UEG}(x,t) = \frac{\pi^2}{6}\rho(x,t)^3$$

while $\partial_x \rho$ and $j$ are both zero.

### C Connecting the opacity parameter $a$ with time

In order to associate time to the opacity parameter $a$, let us first define the range of the opacity parameter, $a$, takes. We want to reach $a_{final} = 0$ starting from a large $a_{\text{initial}} = a(t = 0)$ in a time $\tau$. For simplicity, we assume a linear dependence on time

$$a(t) = a_{\text{initial}}(1 - t/\tau)$$

We can define a constant $v = \dot{a}(t) = a_{\text{initial}}/\tau$. We see that $a_{\text{initial}} = \infty$ is not an acceptable choice if we want $\tau$ to be finite. We now choose $a_{\text{initial}}$ such that the particles in the two half-boxes are just in contact, i.e., the density is of the order of 0.001 atomic units. This value was taken to delimit the shape of the molecules (cf.[10], section 1.1). For a size of the box given by $L = 10$ bohr, chosen to give a reasonable first excited state, this gives $a_{\text{initial}} \approx 40$ atomic units.

We have the freedom to choose $\tau$. For Fig.10, $v = 0.1$, i.e., $\tau = 400$ atomic units≈ 10 femtoseconds.

### D Solving the time-dependent Schrödinger equation

In order to solve Eq.(5) a basis has to be chosen. The basis is given by the functions

$$\chi_k(x, L) = \frac{1}{\sqrt{L}} \cos\left(\frac{(2k-1)\pi}{2L}x\right)$$

that correspond to the symmetric eigenfunctions $u_+$ at $a = 0$. The system of differential equations was solved numerically with Mathematica[16].

The expansion in a fixed basis is complicated by the presence of the time-dependent cusp in $u_+(x = 0)$, as shown in Fig.1. However, this does not seem to affect the discussion of the results.

## References

(1) Messiah, A. *Quantum Mechanics*; North Holland Publishing Company: Amsterdam, The Netherlands, 1967.

(2) Flügge, S. *Practical Quantum Mechanics*; Springer: Berlin, Germany, 1999; p.14.

(3) Wigner, E. *Phys. Rev.* **1934,** *46*, 1002. doi: 10.1103/PhysRev.46.1002

(4) Lewis, G. N. *J. Am. Chem. Soc.* **1916,** *38*, 762. doi: 10.1021/ja02261a002

(5) Durrant, T. R.; Hodgson, M. J. P.; Ramsden, J. D.; Godby, R. W. *arXiv* **2015,** 1505.07687.

(6) Artmann, K. *Z. Naturforschg.* **1946,** *1*, 426.

(7) Scemama, A.; Caffarel, M.; Savin, A. *J. Comput. Chem.* **2007,** *28*, 442. doi: 10.1002/jcc.20526

(8) Lüchow, A.; Petz, R. *J. Comput. Chem.* **2011,** *32*, 2619. doi: 10.1002/jcc.21841

(9) Savin, A. *Reviews of Modern Quantum Chemistry: A Celebration of the Contributions of Robert G. Parr*; Sen, K. D. Ed.; World Scientific: Singapore, 2002; p.43.

(10) Bader, R. F. W. *Atoms in Molecules: A Quantum Theory*; Oxford University Press: Oxford, UK, 1990.

(11) Becke, A. D.; Edgecombe, K. E. *J. Chem. Phys.* **1990,** *92*, 5397. doi: 10.1063/1.458517

(12) Burnus, T.; Marques, M. A. L.; Gross, E. K. U. *Phys. Rev. A* **2005,** *71*, 010501. doi: 10.1103/PhysRevA.71.010501

(13) Sini, G.; Maitre, P.; Hiberty, P. C.; Shaik, S. S. *J. Mol. Struct. THEOCHEM* **1991,** *229*, 163.

(14) Petersilka, M.; Gross, E. *Laser Physics* **1999,** *9*, 1.

(15) Dobson, J. F. *J. Chem. Phys.* **1993,** *98*, 8870. doi: 10.1063/1.464444

(16) Wolfram, S. *Mathematica Edition*, Version 11.1; Wolfram Research, Inc.: Champaign, Illinois, USA, 2017.